

# Energy Efficient A/D Conversion for Sequential Wideband Multichannel Spectrum Sensing in Cognitive Radio Network

Zhengpeng Liu, Yongpan Liu, Huazhong Yang

Electronic Engineering Dept., Tsinghua University, Beijing, 100084, P.R. China

Email: liuzp06@mails.tsinghua.edu.cn, {ypliu,yanghz}@tsinghua.edu.cn

**Abstract**—Cognitive radio (CR) draws lots of attentions due to its efficient spectrum utilization by dynamic spectrum access [1]. Due to hardware limitation, secondary user (SU) always divides the whole wideband into multiple subchannels, senses and accesses sequentially. Since wireless devices are always battery powered, energy efficiency is important. This paper analyzes the optimal parameters of ADCs to improve energy efficiency of the SU in cognitive radio networks (CRN). First, we study the state of the art analog-to-digital converter (ADC) to provide a power model, considering both sampling frequency  $f_s$  and bit resolution  $L_{bit}$ . We then derive the sequential sensing energy optimization problem for ADCs [2] and CRN energy efficiency optimization problem under detection and throughput constraints. Finally, we conclude how to select the optimal parameters for ADCs in CRN.

**Keywords**—Cognitive Radio, Sequential Sensing, Energy Efficiency, Power Model, Analog-to-Digital Converter (ADC)

## I. INTRODUCTION

With the development of wireless communication, spectrum resource is becoming rare. As a result, CR is proposed to overcome the inefficiency of the static spectrum allocation. Spectrum sensing is the key function of cognitive radio. The SU in the CRN carries out spectrum sensing task to identify the spectrum holes [3] by the primary user (PU), and transmits without causing harmful interference to the PU. Spectrum sensing methods can be divided into energy detection, cyclostationary feature detection, matched filter detection, etc. [4]. When it comes to wideband spectrum sensing, there are a number of works from different approaches. Quan et al. [5] proposed multiband joint detection (MJD) framework for wideband sensing, which requires a wideband architecture of the RF front-end. Also wavelet transformation is used to estimate the power spectral density (PSD) of the received signal and the signal is decomposed into multiple nonoverlapping subbands in the frequency domain [6]. However, due to hardware limitation of battery powered wireless devices, our concentration lies on sequential sensing, where secondary user

(SU) divides the whole wideband into multiple subchannels, senses and accesses sequentially [7].

As for the resource allocation and MAC layer optimization which affects the achieved throughput and energy efficiency, Liang et al. [8] studied the fundamental tradeoff between sensing capacity and achievable throughput of the SUs, and the structure of period sensing in CRN was proposed. Since most wireless devices are battery powered, energy efficiency of CRN is becoming a hot topic in recent research. Li et al. [9] studied the optimal transmission duration and power allocation to achieve maximum energy efficiency.

However, none of the above papers considered the effect of practical circuits' parameters on the performance of CRN. Xu et al. [2] considered the effect of ADC sampling frequency on spectrum sensing energy consumption and detection probability of CR. But the power model of ADC proposed was based on a single commercial chip (AD9051 chip set), which could not represent the state of the art ADC design trends. To our best knowledge, [10] is the first to consider the bit quantization effect on spectrum sensing detection performance. However, their network scenario is different from ours. Moreover, they did not consider the effect of ADC bit resolution on power consumption.

We study the parameter choice of ADC sampling frequency and bit resolution for energy efficiency of the SU in CRN. With higher sampling frequency, the bandwidth of each subchannel is expanded. Thus the SU can sequentially sense the total wideband in fewer times. However, higher sampling frequency also results in higher ADC power consumption. Moreover, sampling frequency has an influence on sensing performance. With lower bit resolution, the ADC power consumption can be lower. But lower bit resolution will degrade the sensing performance, which may result in a degradation in SU's throughput. Thus considering the tradeoff between power consumption and transmission throughput, the energy efficiency optimization problem is derived. Our contributions are listed as below:

- We survey the the state of the art ADC designs and acquire a more accurate ADC power model related to CR applications, considering both sampling frequency  $f_s$

This work was supported in part by the NSFC under grant 60976032 and 61204032, High-Tech Research and Development (863) Program under contract 2013AA013201 and National Science and Technology Major Project under contract 2010ZX03006-003-01.

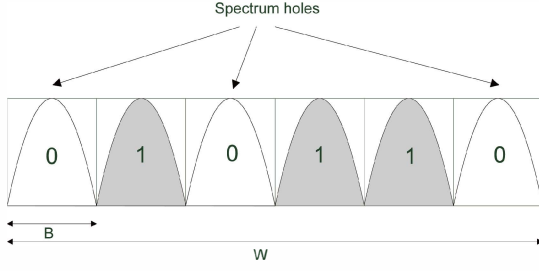


Fig. 1. Frequency structure [11].

and bit resolution  $L_{bit}$ .

- We derive the energy efficiency problem of the SU in CRN with optimization parameters considering ADC sampling frequency, bit resolution under detection and throughput constraints.
- Numerical results show that a high sampling frequency  $f_s$  and 2-4 bit resolution  $L_{bit}$  is more appropriate and energy efficient under most realistic scenarios.

The paper is organized as follows. First, system-level models of CRN are described in Section II. Then, ADC sequential sensing energy optimization problem and CRN energy efficiency optimization problem under detection and throughput constraints are formulated in Section III. Finally, numeric results are showed and discussed in Section IV.

## II. MODELING METHODOLOGY

This section presents a modeling methodology for system-level power and performance analysis of the SU in CRN.

### II.A. CRN Behavior Model

This paper considers a wideband multichannel CRN model with multiple SUs and multiple PUs. The CRN has a star topology and each SU senses and transmits data to the coordinator. Without loss of generality, we focus on the performance of each SU. As parallel wideband spectrum sensing is resource extensive, we assume that each SU deploys sequential sensing [2]. The whole wideband spectrum  $W$  is divided into multiple subchannels with bandwidth  $B$ . Each SU sensed successively in  $N = W/B$  times [2]. The SU system behavior model is similar to [11], SU senses all the subchannels and utilizes all the idle subchannels in an OFDM transmission mode. The spectrum sensing in each subchannel is modeled as a binary hypothesis test, where  $H_{1,i}$  ("1") represents the presence of PU in subchannel  $i$  and  $H_{0,i}$  ("0") represents that SU can access subchannel  $i$ . Figure 1 shows the frequency structure.

Each SU senses and transmits in a periodic sensing manner [8] in Figure 2. Each frame  $T$  is divided into sensing phase  $\tau$  and transmitting phase  $T - \tau$ . The sensing phase  $\tau$  consists of  $N$  subslots  $\sum_{i=1}^N \tau_{si}$ , where  $\tau_{si}$  is the sensing subslot on subchannel  $i$ . Uniform sensing durations  $\tau_{s1} = \dots = \tau_s$  are assumed and  $\tau = N\tau_s$ .

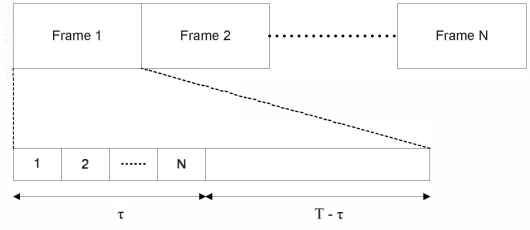


Fig. 2. Sequential period sensing frame structure [11].

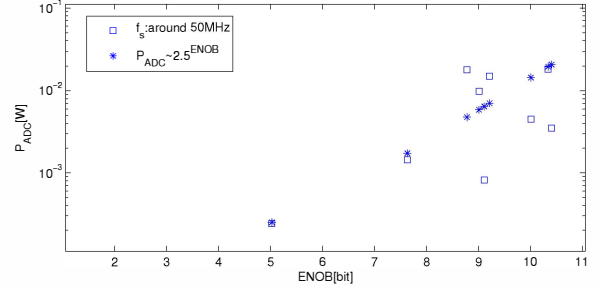


Fig. 3. Power vs. ENOB of ADCs supporting sampling frequency of 50MHz.

For simplicity [2], we assume that there are no correlations among subchannels and the PU activity in each subchannel follows an independent identically distributed ON/OFF activity model. PU's average ON/OFF duration is assumed to be much longer than the SU's frame  $T$ . PU will be present in the channel with probability  $Pr(H_1)$  and absent with probability  $Pr(H_0) = 1 - Pr(H_1)$ .

### II.B. SU Power Model

The power consumption of the SU in CRN can be derived as  $P_{total} = P_{sense} + P_{tx}$ , where  $P_{tx}$  is the transmitting power and  $P_{sense} = P_{ADC} + P_{RF,SAC}$  is the spectrum sensing power consisting of ADC power  $P_{ADC}$  and RF components, sensing circuit power  $P_{RF,SAC}$ .

**II.B.1) ADC Power:** ADC's design complexity as well as power consumption will grow with its sampling frequency  $f_s$  and its bit resolution  $L_{bit}$ . We adopt a similar ADC power model in [12]. Different from the power model in [2], we emphasize that the ADC is always designed to operate on the maximum sampling frequency instead of lower frequency. The survey of the state of the art designs are mainly based on [13]. Attentions are paid to the most relevant designs with similar characteristics, i.e., ADCs with sampling frequency from 1 MHz to 100 MHz and effective number of bits (ENOB)<sup>1</sup> below 11 bit within the last six years (from 2006 to 2012).

Figure 3 and Figure 4 show the power consumption of ADCs in relation to ENOB and sampling frequency. For the largest subset of the surveyed ADCs, where the sampling

<sup>1</sup>ENOB is an effective quantization resolution that accounts for hardware impairment. It is typically 0.5 to 1.5 bits below the nominal resolution. For simplicity, we assume ADC bit resolution  $L_{bit} = \text{ENOB}$ .

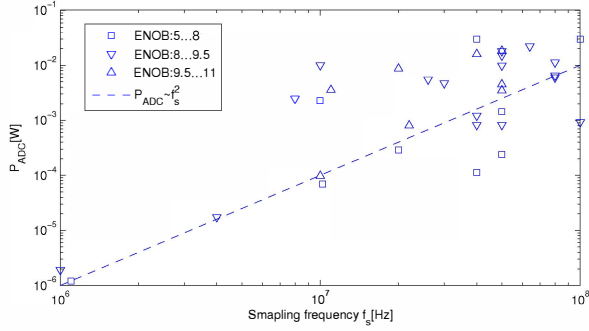


Fig. 4. Power vs. sampling frequency of ADCs with ENOB ranging from 5 to 11.

frequency is around 50 MHz, it can be observed that the power consumption scales with  $2.5^{ENOB}$ . Similarly, when the ENOB is restricted, the power consumption scales with  $f_s^2$ . Thus the proportional relation of the state of the art ADCs with sampling frequency between 1 MHz and 100 MHz can be got as:  $P_{ADC} \propto 2.5^{ENOB} \cdot f_s^2$ . The sample-and-hold noise limit of ADC is given as:  $P_{ADC} \propto 2^{ENOB} \cdot f_s^2$ . The slight difference implies that the power consumption of today's designs is still more increasing with ENOB and sampling frequency than the fundamental limit suggests.

Therefore we have ADC power model  $P_{ADC} = c_{ADC} \cdot 2.5^{ENOB} \cdot f_s^2$ , where  $c_{ADC}$  is a constant given by curve fitting.

**II.B.2) RF and Sensing Algorithm Circuitry:** Since limited work on the whole CR system's application specific integrated circuit (ASIC) implementation has been published, for RF and sensing circuit, we just estimate the power with typical values [14] and assume the power consumption as constant regardless of sampling frequency  $f_s$  or bit resolution  $L_{bit}$ . This is reasonable since RF components are mainly working on radio frequency (RF) instead of intermediate frequency (IF) which relates to  $f_s$ . The power of sensing circuit is given as  $P_{SAC}$  [15]. RF components' power is  $P_{RF}$  [15], consisting of the low noise amplifier (LNA), the voltage controlled oscillator (VCO), the phase-locked loop (PLL), mixers and filters. Then the total power of RF and sensing circuit is  $P_{RF,SAC} = P_{RF} + P_{SAC}$ .

**II.B.3) Transmitting Power:** The transmitting power can be estimated as [16]:  $P_{tx} = \frac{\xi}{\zeta} P_t + P_{ct}$ , where  $\xi$  is the peak-to-average ratio (PAR) of the RF power amplifier (PA),  $\zeta$  is the drain efficiency,  $P_t$  is transmitting signal power, and  $P_{ct}$  is the power consumed in various transmit circuits excluding the PA power. The well-known Shannon-Hartley theorem [17] is given as:

$$\begin{aligned} R &= B \log_2(1 + \text{SNR}_{SU,tx}) = B \log_2(1 + g \text{SNR}_{SU,tx}) \\ &= B \log_2\left(1 + \frac{g P_t}{N_0 B}\right) \quad (1) \end{aligned}$$

We assume that SU fixes transmitting side signal-to-noise ratio  $\text{SNR}_{SU,tx}$  for different bandwidth  $B$ . Given the bandwidth  $B$ , channel propagation loss  $g$ , one-sided noise spectral

level  $N_0$ , the transmitting rate  $R$  can be estimated. Transmitting signal power  $P_t$  can be got as  $P_t = \text{SNR}_{SU,tx} N_0 B$ . And  $P_{ct}$  is independent of transmission rate and can be considered as a constant [16].

## II.C. SU Sensing Performance Model

As explained in subsection II-A, the binary hypothesis test for spectrum sensing in each subchannel is:

$$\begin{aligned} H_{0,i} : r_i(k) &= n_i(k) \\ H_{1,i} : r_i(k) &= s_i(k) + n_i(k), i = 1, 2, \dots, N \end{aligned} \quad (2)$$

The intermediate frequency (IF) signal within bandwidth  $B$  is sampled at Nyquist sampling rate  $f_s = B$ . Then as derived in most papers on CR [8], the noise  $n_i(k)$  is real-valued additive white Gaussian noise with mean zero and variance  $\mathbb{E}[|n_i(k)|^2] = \sigma_n^2 = N_0 B$ . Primary signal  $s_i(k)$  is also real-valued Gaussian with mean zero and variance  $\mathbb{E}[|s_i(k)|^2] = \sigma_s^2$  [8].

Energy detection spectrum sensing method is performed, and decision statistic on channel  $i$  is given by  $T_i(r) = \frac{1}{M_i} \sum_{k=1}^{M_i} |\tilde{r}_i(k)|^2$ , where  $M_i = \tau_{si} f_s$  represents the number of samples for sensing on channel  $i$  and  $\tilde{r}_i(k)$  is the ADC quantization result of  $r_i(k)$ .

The ADC resolution quantization effect on spectrum sensing can be analyzed as follows: ADC has input amplitude dynamic range  $[-W_{ap}, W_{ap}]$  and bit resolution  $L_{bit}$ , thus step size  $\Delta = 2W_{ap}/2^{L_{bit}}$ . Quantization introduces noise  $q$  with variance  $\sigma_q^2 = \Delta^2/12$  [18]. When hypothesis  $H_{1,i}$  holds, the received signal before ADC is real-valued Gaussian with mean zero and variance  $\sigma_s^2 + \sigma_n^2$ , and  $\sigma_n^2$  for  $H_{0,i}$ . After quantization,  $\tilde{r}_i(k) = r_i(k) + q_i(k)$ . Different from the derivation in [10], we emphasize that SU has spectrum sensing errors when distinguishing  $H_{1,i}$  from  $H_{0,i}$  and it is not appropriate to assume different dynamic range bound for a running ADC. Since the standard deviation of a Gaussian is 1/3 of the peak value, the ADC amplitude dynamic range is fixed to  $W_{ap} = 3 \times \sqrt{\sigma_s^2 + \sigma_n^2}$  and  $\sigma_q^2 = W_{ap}^2 / (3 \times (2^{L_{bit}})^2)$ . Uniform SNR and sensing duration  $\tau_{si}$  is assumed on different subchannels, and the spectrum sensing threshold is set all the same to  $\lambda$ . The detection probability and false alarm probability are the same on different subchannels and calculated a slight different from [10]:

$$\begin{aligned} P_f &= P(T_i(r) > \lambda | H_{0,i}) = Q\left(\frac{\lambda - \mu_0}{\sigma_0}\right) \\ P_d &= P(T_i(r) > \lambda | H_{1,i}) = Q\left(\frac{\lambda - \mu_1}{\sigma_1}\right) \end{aligned} \quad (3)$$

where  $Q(\cdot)$  is the complementary cumulative distribution function and  $\mu_0, \sigma_0, \mu_1, \sigma_1$  represent the expectation and

standard deviation of  $T_i(r)$  under the binary hypothesis:

$$\begin{aligned}\mu_0 &= \sigma_n^2 + \sigma_q^2 \\ \sigma_0 &= \sqrt{2(\sigma_n^2 + \sigma_q^2)^2/M} \\ \mu_1 &= \sigma_s^2 + \sigma_n^2 + \sigma_q^2 \\ \sigma_1 &= \sqrt{2(\sigma_s^2 + \sigma_n^2 + \sigma_q^2)^2/M} \quad (M = \tau_s f_s)\end{aligned}\quad (4)$$

### III. FORMULATION

This section describes ADC sequential sensing energy optimizing problem under detection constraints, and CRN energy efficiency optimizing problem under detection and throughput constraints.

#### III.A. ADC Sequential Sensing Energy Optimization

The goal is to minimize the energy consumption of ADC sequential sensing  $E_{ss}(f_s, L_{bit})$  under detection constraints [2].  $P_{f,th}$ ,  $P_{d,th}$  are spectrum sensing false alarm probability threshold and detection probability threshold,  $\tau_s$  is predefined in this problem.

$$\begin{aligned}\text{Minimize} \quad & E_{ss}(f_s, L_{bit}) \\ \text{subject to} \quad & P_f(f_s, L_{bit}, \lambda) \leq P_{f,th} \\ \text{and} \quad & P_d(f_s, L_{bit}, \lambda) \geq P_{d,th}\end{aligned}$$

The optimization variables for this problem are ADC sampling frequency  $f_s$ , bit resolution  $L_{bit}$  and sensing decision threshold  $\lambda$ . The total energy consumption  $E_{ss}(f_s, L_{bit})$  is derived as [2]

$$E_{ss}(f_s, L_{bit}) = NP_{ADC}\tau_s = W\tau_s \frac{P_{ADC}(f_s, L_{bit})}{f_s} \quad (5)$$

Using Equation 3, the detection constraints of this problem can be simplified as:

$$Q^{-1}(P_{f,th})\sigma_0 - Q^{-1}(P_{d,th})\sigma_1 \leq \sigma_s^2 \quad (6)$$

where  $Q^{-1}(\cdot)$  is the inverse function of  $Q$  function. Equation 6 gives the feasible region of  $f_s$  and  $L_{bit}$ , which is the gray area with star line boundary shown in Figure 5.

The objective function  $E_{ss}(f_s, L_{bit})$  decreases with smaller  $f_s$  or  $L_{bit}$ , so the optimal point is on the feasible region boundary, which can be easily found by one dimension search algorithm.

#### III.B. CRN Energy Efficiency Optimization

The energy efficiency of the CRN is defined as:

$$\eta_{CRN}(f_s, L_{bit}, \tau, \lambda) = \frac{Th_{CRN}(f_s, L_{bit}, \tau, \lambda)}{E_{CRN}(f_s, L_{bit}, \tau, \lambda)} \quad (7)$$

where  $Th_{CRN}(f_s, L_{bit}, \tau, \lambda)$  is the average throughput of the SU in CRN and  $E_{CRN}(f_s, L_{bit}, \tau, \lambda)$  is the energy consumption. The formulation of the CRN energy efficiency optimization problem under detection and throughput constraints

TABLE I  
FOUR CASES BETWEEN THE ACTIVITIES OF PU AND SU IN ONE SUBCHANNEL

Cases	Probability	Energy	Throughput
i	$P_1 = P_r(H_1)P_d$	$(P_{ADC} + P_{RF,SAC})\tau_s$	0
ii	$P_2 = P_r(H_0)P_f$	$(P_{ADC} + P_{RF,SAC})\tau_s$	0
iii	$P_3 = P_r(H_1)(1 - P_d)$	$(P_{ADC} + P_{RF,SAC})\tau_s + P_{tx}(T - \tau)$	0
iv	$P_4 = P_r(H_0)(1 - P_f)$	$(P_{ADC} + P_{RF,SAC})\tau_s + P_{tx}(T - \tau)$	$R(T - \tau)$

follows:

$$\begin{aligned}\text{Maximize} \quad & \eta_{CRN}(f_s, L_{bit}, \tau, \lambda) \\ \text{subject to} \quad & P_f(f_s, L_{bit}, \tau, \lambda) \leq P_{f,th} \\ \text{and} \quad & P_d(f_s, L_{bit}, \tau, \lambda) \geq P_{d,th} \\ \text{and} \quad & Th_{CRN}(f_s, L_{bit}, \tau, \lambda) \geq Th_{CRN,th}\end{aligned}$$

The throughput threshold of CRN is  $Th_{CRN,th} = P_r(H_0)(1 - P_{f,th})W \log_2(1 + g\text{SNR}_{SU,tx})\eta_T T$ . We maximize the energy efficiency  $\eta_{CRN}$  with optimization variables: ADC sampling frequency  $f_s$ , bit resolution  $L_{bit}$ , sensing decision threshold  $\lambda$  and sensing phase length  $\tau$ . Detection constraints are set for the protection of PUs.  $Th_{CRN,th}$  is the minimal required throughput of the CRN, since maximal energy efficiency is meaningful only if a certain amount of throughput is ensured.

$Th_{CRN}(f_s, L_{bit}, \tau, \lambda)$  and  $E_{CRN}(f_s, L_{bit}, \tau, \lambda)$  are derived as follows: there are four possible cases between the activities of the PUs and the SUs [19]. Take the activities of the PU and the SU in one subchannel for example: In case i, when the PU is present and SU detects correctly, no data will be transmitted and the energy consumption of SU is  $(P_{ADC} + P_{RF,SAC})\tau_s$ . In case ii, the PU is absent but SU detects it as present, no data will be transmitted and energy consumption is  $(P_{ADC} + P_{RF,SAC})\tau_s$ . In case iii, the PU is present but SU miss detects it, SU will transmit and collide with PU's packet. In this case, the throughput gain is zero and the energy consumption is  $(P_{ADC} + P_{RF,SAC})\tau_s + P_{tx}(T - \tau)$ . In case iv, SU successfully detects PU's absence and transmits after sensing, the throughput gain is  $R(T - \tau)$  and energy is  $(P_{ADC} + P_{RF,SAC})\tau_s + P_{tx}(T - \tau)$ . The throughput and energy consumption under different cases are summarized in Table I. As a result,  $Th_{CRN}(f_s, L_{bit}, \tau, \lambda)$  and  $E_{CRN}(f_s, L_{bit}, \tau, \lambda)$  of the SU in CRN are:

$$\begin{aligned}Th_{CRN}(f_s, L_{bit}, \tau, \lambda) &= P_4NR(T - \tau) \\ &= P_r(H_0)(1 - P_f)NR(T - \tau)\end{aligned} \quad (8)$$

$$\begin{aligned}E_{CRN}(f_s, L_{bit}, \tau, \lambda) &= P_1N(P_{ADC} + P_{RF,SAC})\tau_s + \\ &P_2N(P_{ADC} + P_{RF,SAC})\tau_s + \\ &P_3N(P_{ADC} + P_{RF,SAC})\tau_s + P_{tx}(T - \tau) + \\ &P_4N(P_{ADC} + P_{RF,SAC})\tau_s + P_{tx}(T - \tau) \\ &= (P_{ADC} + P_{RF,SAC})\tau + \\ &(1 - P_r(H_1)P_d - P_r(H_0)P_f)NP_{tx}(T - \tau)\end{aligned} \quad (9)$$

TABLE II  
PARAMETERS FOR SIMULATION

Parameter	Value
Total bandwidth of spectrum $W$	240 MHz
One-sided noise spectral level $N_0$	-173 dBm/Hz
Received PU signal SNR before quantization $\gamma = \sigma_s^2/\sigma_n^2$	-21 dB
PU present probability $Pr(H_1)$	0.4
SU's frame length $T$	100 ms
SU's transmitting side signal-to-noise ratio $SNR_{SU,tx}$	106 dB
Channel propagation loss $g$	-70 dB
SU's spectrum sensing detection probability threshold $P_{d,th}$	0.9
SU's false alarm probability threshold $P_{f,th}$	0.1
Numerical value related to the throughput threshold $\eta_T$	10%
PAR of the RF power amplifier $\xi$	6 dB
Drain efficiency of the RF power amplifier $\zeta$	0.35
Numerical value related to ADC power model $c_{ADC}$	$5.64 \times 10^{-22}$
Power of the sensing algorithm circuitry $P_{SAC}$	23.75 mW [15]
Power of the RF components $P_{RF}$	90.9 mW [15]
Numerical value related to transmitting power model $P_{ct}$	210 mW [16]

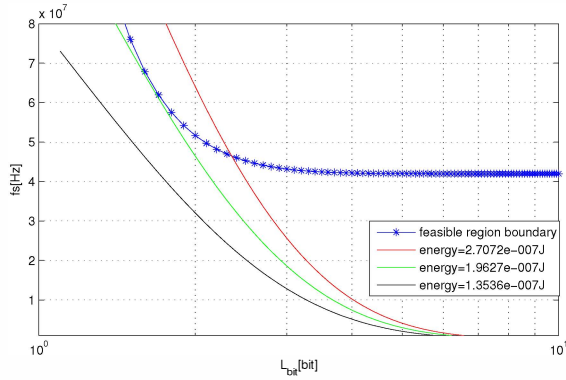


Fig. 5. ADC sequential sensing energy optimization.

This optimization problem is a nonlinear optimization problem. It is general and nonconvex and the optimal point is found using MATLAB numerical simulation.

#### IV. NUMERICAL RESULTS

In this section, we first propose the optimization numeric results for the ADC sequential sensing energy optimization problem and discuss the results for energy efficiency optimization problem of CRN. The numerical results are given by MATLAB simulation and parameters for simulation are summarized in Table II.

##### IV.A. ADC Sequential Sensing Energy Optimization

Subchannel sensing duration  $\tau_s$  is predefined to 5 ms in this optimization problem. As in Figure 5, a curve represents a fixed total sequential sensing energy  $E_{ss}(f_s, L_{bit})$  with different  $f_s$  and  $L_{bit}$ , and the three different color of curve represents different  $E_{ss}$ . It can be observed that  $E_{ss}$  decreases with smaller  $f_s$  or  $L_{bit}$ , which can be concluded from Equation 5. When  $L_{bit} \geq 3$  bit, the effect of  $L_{bit}$  on  $P_d$ ,  $P_f$  thus on feasible region is quite small. The boundary of  $f_s$  is almost constant 42 MHz, which is limited by  $\gamma$  and  $\tau_s$ . When  $L_{bit}$  goes down below 3 bit, the loss in sensing performance

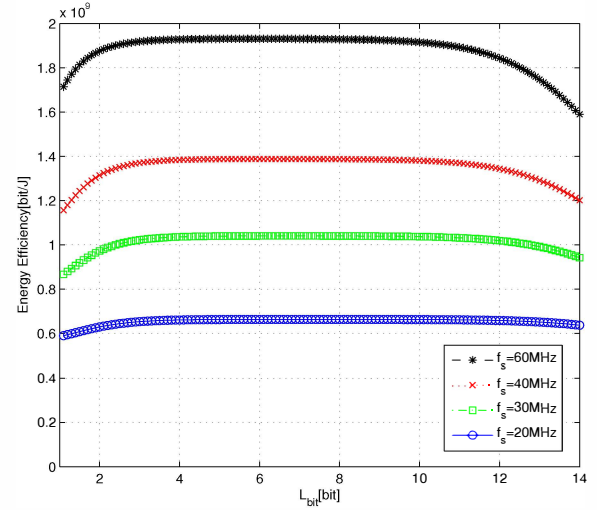


Fig. 6. CRN energy efficiency vs. bit resolution  $L_{bit}$  of ADC.

caused by  $L_{bit}$  has to be gained by larger number of samples, and higher  $f_s$  is required.

The optimal point for minimizing  $E_{ss}$  is searched on the feasible region boundary and the minimum ADC sequential sensing energy is  $E_{ss,min} = 1.989 \times 10^{-7}$  J when  $L_{bit} = 1.7$  bit,  $f_s = 61.08$  MHz. This indicates that the decrease of energy consumption by lower  $L_{bit}$  outweighs the energy consumption of higher  $f_s$  for guaranteeing sensing performance.

It should be emphasized that the feasible region of  $f_s$  and  $L_{bit}$  is highly influenced by the predefined value of received PU signal SNR  $\gamma$  and sensing duration  $\tau_s$ . Our work is just to provide a methodology to optimize the problem, and the optimal  $f_s$ ,  $L_{bit}$  may differ in systems with different parameters.

##### IV.B. CRN Energy Efficiency Optimization

The sampling frequency  $f_s$  is restricted to  $1 \text{ MHz} \sim 60 \text{ MHz}$  and bit resolution  $L_{bit}$  is  $1 \sim 14$  bit. Solved by MATLAB, the maximum  $\eta_{CRN}$  is  $1.9432 \times 10^4$  bit/J when  $L_{bit} = 6.5$  bit,  $f_s = 60$  MHz,  $\tau = 28.4$  ms,  $\lambda = 3.0177 \times 10^{-13}$  V<sup>2</sup>.

Besides searching for global maximum  $\eta_{CRN}$  under constraints, the achieved maximum  $\eta_{CRN}$  under different  $f_s$  and  $L_{bit}$  is also showed in Figure 6 and Figure 7. Intuitively observed from Table I, the probability of case iv  $P_4$  should be larger to achieve higher  $\eta_{CRN}$ , and  $P_3$  should be smaller than  $P_1$ . For simplicity, we relax the constraints and assume constant false alarm rate (CFAR).

From Figure 6, when  $L_{bit}$  is  $3 \sim 10$  bit,  $\eta_{CRN}$  is almost constant and the difference is quite small, since the increase of  $L_{bit}$  has little effect on sensing performance when  $L_{bit} \geq 3$  [10] and  $P_{ADC}$  is still relatively small compared to  $P_x$ . If  $L_{bit} \geq 10$ , the degradation in  $\eta_{CRN}$  can be observed because ADC with  $L_{bit} \geq 10$  consumes too much energy



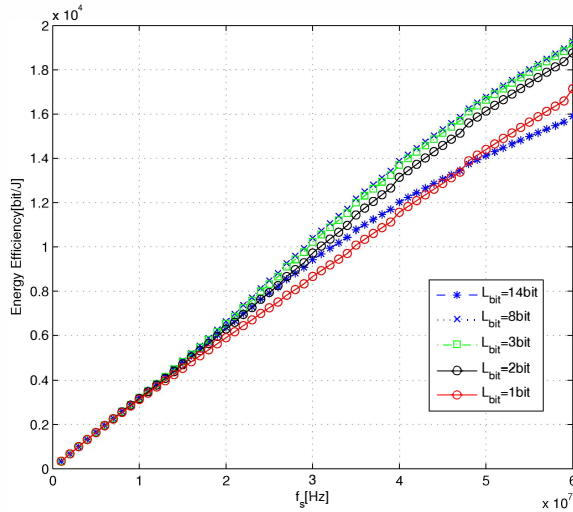


Fig. 7. CRN energy efficiency vs. sampling frequency  $f_s$  of ADC.

exponentially compared to  $P_{tx}$  while providing little improvement in sensing performance. As to  $L_{bit} \leq 3$ , with sensing performance decreasing,  $Th_{CRN}$  decreases faster than  $E_{CRN}$ , which results in the degradation in  $\eta_{CRN}$ . For  $L_{bit} = 2$ ,  $\eta_{CRN}$  is just 2.8% ( $f_s = 60$  MHz)  $\sim$  5.2% ( $f_s = 20$  MHz) smaller than the maximum value, which implies that  $L_{bit} = 2$  is acceptable. This conclusion can also be drawn from Figure 7. Figure 7 also demonstrates that  $\eta_{CRN}$  monotonically increases with sampling frequency  $f_s$ . This is due to the fact that  $Th_{CRN}$  changes little with  $f_s$ . And with higher  $f_s$  in 1 MHz  $\sim$  60 MHz, the decrease of  $E_{CRN}$  caused by higher sensing performance still outweighs the increase of  $E_{CRN}$  caused by larger  $P_{ADC}$  because  $P_{tx}$  is still relatively larger.

From the numerical results, we conclude that in order to guarantee high energy efficiency of the CRN, a high sampling frequency  $f_s$  of ADC is better, and since higher bit resolution ADC is more difficult to design, bit resolution  $L_{bit} = 2 \sim 4$  bit is appropriate.

## V. CONCLUSIONS

This work has analyzed the optimal parameters  $f_s$  and  $L_{bit}$  of ADC for energy efficiency of the SU in CRNs. Models of a CRN are given, and ADC power model is derived through surveying recently works [13]. The ADC sequential sensing optimization problem under detection constraints is studied first. Next, we combine the energy consumption with sensing performance and study the CRN energy efficiency optimization problem under detection and throughput constraints. Numerical results show that a high sampling frequency  $f_s$  and low bit resolution  $L_{bit}$  is usually more appropriate and energy efficient for the SU in CRN under proposed parameters. More accurate analysis and CR system modeling have to be left for future research. And more complex scenarios of CRN such as PU with different traffic distributions can also be covered.

## REFERENCES

- [1] I. Akyildiz, W. Lee, M. Vuran, and S. Mohanty, "Next generation/dynamic spectrum access/cognitive radio wireless networks: a survey," *Computer Networks*, vol. 50, no. 13, pp. 2127–2159, 2006.
- [2] M. Xu, H. Li, and X. Gan, "Energy efficient sequential sensing for wideband multi-channel cognitive network," in *Communications (ICC), 2011 IEEE International Conference on*. IEEE, 2011, pp. 1–5.
- [3] R. Tandra, A. Sahai, and S. Mishra, "What is a spectrum hole and what does it take to recognize one?" *Proceedings of the IEEE*, vol. 97, no. 5, pp. 824–848, 2009.
- [4] L. Lu, X. Zhou, U. Onunkwo, and G. Li, "Ten years of research in spectrum sensing and sharing in cognitive radio," *EURASIP Journal on Wireless Communications and Networking*, vol. 2012, no. 1, p. 28, 2012.
- [5] Z. Quan, S. Cui, A. Sayed, and H. Poor, "Optimal multiband joint detection for spectrum sensing in cognitive radio networks," *Signal Processing, IEEE Transactions on*, vol. 57, no. 3, pp. 1128–1140, 2009.
- [6] Z. Tian and G. Giannakis, "A wavelet approach to wideband spectrum sensing for cognitive radios," in *Cognitive Radio Oriented Wireless Networks and Communications, 2006. 1st International Conference on*. IEEE, 2006, pp. 1–5.
- [7] A. Sahai and D. Cabric, "A tutorial on spectrum sensing: Fundamental limits and practical challenges," in *Proc. IEEE Int. Symp. New Frontier in Dyn. Spectrum Access Netw. (DySPAN)*. IEEE, 2005.
- [8] Y. Liang, Y. Zeng, E. Peh, and A. Hoang, "Sensing-throughput tradeoff for cognitive radio networks," *Wireless Communications, IEEE Transactions on*, vol. 7, no. 4, pp. 1326–1337, 2008.
- [9] L. Li, X. Zhou, H. Xu, G. Li, D. Wang, and A. Soong, "Energy-efficient transmission in cognitive radio networks," in *Consumer Communications and Networking Conference (CCNC), 2010 7th IEEE*. IEEE, 2010, pp. 1–5.
- [10] H. Chen, C. Tse, and F. Zhao, "Optimal quantisation bit budget for a spectrum sensing scheme in bandwidth-constrained cognitive sensor networks," *Wireless Sensor Systems, IET*, vol. 1, no. 3, pp. 144–150, september 2011.
- [11] P. Paysarvi-Hoseini and N. Beaulieu, "Sequential multichannel joint detection framework with non-uniform channel sensing durations for cognitive radio networks," in *Communications (ICC), 2011 IEEE International Conference on*. IEEE, 2011, pp. 1–6.
- [12] S. Krone and G. Fettweis, "Energy-efficient a/d conversion in wideband communications receivers," in *Vehicular Technology Conference (VTC Fall), 2011 IEEE*. IEEE, 2011, pp. 1–5.
- [13] B. Murmann, "Adc performance survey 1997-2012." [Online]. Available: <http://www.stanford.edu/~murmann/adcsurvey.html>
- [14] W. Gabran, P. Pawelczak, and D. Cabric, "Multi-channel multi-stage spectrum sensing: Link layer performance and energy consumption," in *New Frontiers in Dynamic Spectrum Access Networks (DySPAN), 2011 IEEE Symposium on*. IEEE, 2011, pp. 164–172.
- [15] T. Song, J. Park, S. Lee, J. Choi, K. Kim, C. Lee, K. Lim, and J. Laskar, "A 122-mw low-power multiresolution spectrum-sensing ic with self-deactivated partial swing techniques," *Circuits and Systems II: Express Briefs, IEEE Transactions on*, vol. 57, no. 3, pp. 188–192, 2010.
- [16] Y. Pei, Y. Liang, K. Teh, and K. Li, "Energy-efficient design of sequential channel sensing in cognitive radio networks: Optimal sensing strategy, power allocation, and sensing order," *Selected Areas in Communications, IEEE Journal on*, vol. 29, no. 8, pp. 1648–1659, 2011.
- [17] C. Shannon, "A mathematical theory of communication," *ACM SIGMOBILE Mobile Computing and Communications Review*, vol. 5, no. 1, pp. 3–55, 2001.
- [18] Q. Ying, Y. Feng, and W. Dou, *Discrete-time signal analysis and processing*. Tsinghua University Press, 2001.
- [19] E. Peh, Y.-C. Liang, Y. L. Guan, and Y. Pei, "Energy-efficient cooperative spectrum sensing in cognitive radio networks," in *Global Telecommunications Conference (GLOBECOM 2011), 2011 IEEE*. IEEE, 2011, pp. 1–5.